



HAL
open science

Silver-doped rutile TiO₂ nanotubes synthesis. First insights into selective photo-oxidation of benzyl alcohol derivatives under visible light.

Oriane Delaunay, Audrey Denicourt-Nowicki, Alain Roucoux

► To cite this version:

Oriane Delaunay, Audrey Denicourt-Nowicki, Alain Roucoux. Silver-doped rutile TiO₂ nanotubes synthesis. First insights into selective photo-oxidation of benzyl alcohol derivatives under visible light.. Nano Select, In press, 10.1002/nano.202400056 . hal-04537713

HAL Id: hal-04537713

<https://hal.science/hal-04537713v1>

Submitted on 8 Apr 2024

HAL is a multi-disciplinary open access archive for the deposit and dissemination of scientific research documents, whether they are published or not. The documents may come from teaching and research institutions in France or abroad, or from public or private research centers.

L'archive ouverte pluridisciplinaire **HAL**, est destinée au dépôt et à la diffusion de documents scientifiques de niveau recherche, publiés ou non, émanant des établissements d'enseignement et de recherche français ou étrangers, des laboratoires publics ou privés.

Silver-doped rutile TiO₂ nanotubes synthesis. First insights into selective photo-oxidation of benzyl alcohol derivatives under visible light.

Oriane Delaunay, Audrey Denicourt-Nowicki*, and Alain Roucoux*

Univ Rennes, Ecole Nationale Supérieure de Chimie de Rennes,

CNRS, ISCR – UMR6226, F- 35000 Rennes, France.

E-mails: audrey.denicourt@ensc-rennes.fr; alain.roucoux@ensc-rennes.fr

Abstract

The synergistic effect between rutile TiO₂ nanotubes and silver nanoparticles on the surface was studied. For that purpose, rutile TiO₂ nanotubes were elaborated by an hydrothermal method, doped with silver by a wetness impregnation approach and fully characterized. The as synthesized material showed an improved photocatalytic activity, compared with bare rutile nanotubes, which was correlated to the changes in the optical, structural, and textural properties associated with the variation of silver amount. The photocatalytic activity of the as-prepared catalysts was evaluated into the oxidation of different benzyl alcohol derivatives under visible light.

Introduction

Among all transition-metal oxides and owing to its relevant properties (low cost, abundance, chemical and physical stability, etc.), titanium dioxide (TiO₂) is one of the more relevant semiconductor materials, thus finding applications in a wide range of fields, such as next-generation solar-cell materials or in photocatalysis (for instance, removal of pollutants, CO₂ reduction into energy fuels or water splitting).^[1,2] However, its use is limited not only by its relatively large bandgap (3-3.2 eV), which limits the adsorption of only UV light but also the fast recombination of electron-holes (10⁻¹² to 10⁻¹¹ s).^[2] These limitations could be addressed through morphological modifications, crystal size and geometries of the support such as spherical, hollow, nanotubes (NTs) or nanosheets structures.^[3] For instance, one-dimensional TiO₂ nanotubes will allow to enhance properties like the specific surface area, extending the light absorption as well as an efficient separation of electrons/holes,^[4] thus boosting the photocatalytic performances owing to an improved transport of the charge carriers.^[5,6] An alternative that is also used to improve the catalytic efficiency of the TiO₂ photocatalyst is the doping with a judiciously chosen metal, which lowers the band gap energy by

formation of a Schottky barrier and enhances the participation of the photogenerated holes and electrons in the photocatalytic reactions.^[7-9] Among the noble metals, silver is an attractive candidate due to its great catalytic activity, its nontoxicity and its suitability for industrial applications owing to its relatively low price and the ease to prepare the Ag/TiO₂ composite.^[10] The activity of the Ag/TiO₂ catalyst will depend on different parameters such as the amount and structure of the metal, the morphology of the semiconductor, or the contact and interfaces between silver and TiO₂.

Herein, rutile nanotubes were synthesized *via* an hydrothermal approach and doped with silver by wetness impregnation methodology. This one-dimensional structure was fully characterized by adapted techniques (XRD, TEM, ICP-OES, BET, and UV-visible analyses). In the drive towards more eco-responsible chemical processes, the rutile form was chosen, being more selective than its anatase analog in the oxidation of benzyl alcohol derivatives into the corresponding aldehydes^[11] and avoiding over-oxidation of the products.^[12] The physicochemical properties of the as-prepared catalysts were studied. The photocatalytic selective oxidation of benzyl alcohol, is used as a model reaction to study the influence of the material morphology as well as the metal loading. The best conditions were further extended to benzyl alcohol derivatives.

Results and Discussion

Characterization of Ag-doped Rutile NT

Rutile nanotubes have been easily produced by a simple and environmentally-friendly hydrothermal method and doped with several amounts of silver through the low-cost incipient wetness impregnation approach.

X-Ray Diffraction

Bare rutile nanotubes and 1% silver-doped rutile nanotubes (1% Ag-RNT) were first characterized by X-ray diffraction, and the XRD patterns are displayed in Figure 1. The major diffraction peaks at 2θ values of 27.3°, 36.1°, 41.2° and 54.1° are ascribed to (110), (101), (111), and (211) facets of rutile phase TiO₂, in agreement with the standard spectrum JCPDS n° 88-1175. No peaks from an anatase phase were observed. The XRD pattern of the silver-doped sample is similar to that of the undoped TiO₂ sample. Peaks corresponding to a silver phase were not found in any of the XRD patterns of the composites, probably owing to the good dispersion of the isolated Ag nanoparticles within the TiO₂ nanotubes and also to their low concentration, probably below the detection limit of XRD analysis.

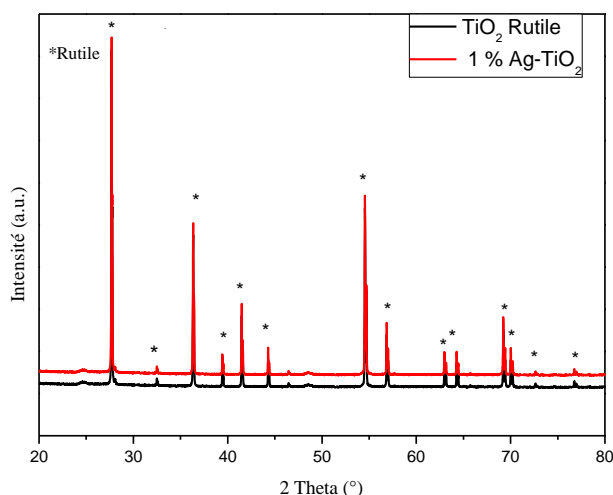


Figure 1. XRD patterns of the prepared rutile TiO₂ nanotubes (black line) and 1% Ag-RNT (red line) photocatalysts.

ICP-OES, BET, and UV-visible analyses

The metal loading was determined by ICP-OES and summarized in Table 1. The impact of silver nanoparticles (NPs) on the specific surface area of the rutile NTs, which was determined from the nitrogen adsorption-desorption isotherms, seems negligible (Table 1). However, the 1% Ag-RNT catalyst presents the higher BET value of 65 m².g⁻¹, compared to 50 m².g⁻¹ for the bare rutile material (Entry 3). For the 1.5% Ag-RNT (Entry 4), the specific surface area starts to decline, likely due to the blocking of the TiO₂ pores by Ag NPs at higher loadings.^[13,14]

Table 1. Silver content and BET specific surface area of x% Ag-RNT photocatalysts.

Entry	Catalyst	Theoretical silver content (wt%)	Measured silver content (wt%) ^[a]	BET (m ² .g ⁻¹) ^[b]
1	RNT	-	-	50
2	0.5% Ag-RNT	0.5	0.31(+/- 0.03)	55
3	1% Ag-RNT	1	1.01(+/- 0.02)	65
4	1.5% Ag-RNT	1.5	1.22(+/- 0.03)	60

[a] Measured by ICP-OES. [b] Determined from nitrogen adsorption-desorption isotherms.

The electronic structure of the as prepared materials that allows to give information on the optical properties (*e.g.*, absorption and band gap) through the irradiating light intensity was determined by UV-visible spectral analysis (Figure 2). On the absorption spectra, all the prepared photocatalysts show an intense absorption edge at 410 nm, which is characteristic of the Ti-O

electron transition. The band gap energies of the materials were estimated using Kubelka-Munk method based on the diffuse reflectance spectrum (Table 2). The bare rutile NTs material shows a band gap of 2.91 eV, lower than that reported for bulk TiO₂ (3 eV)^[15], thus showing a higher potential for visible light absorption. Doping with silver had no significant impact on the bandgap value, probably due to the deposition of Ag on the TiO₂ surface only, and not into the crystal lattice.^[6]

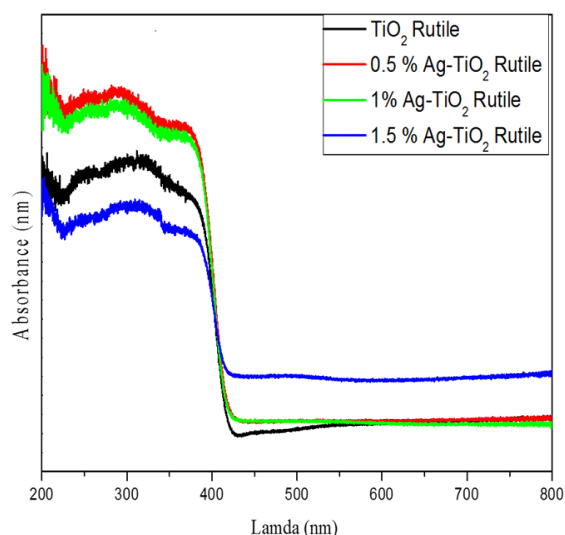


Figure 2. UV-visible absorbance spectra of the synthesized bare rutile nanotubes (black line), 0.5% Ag-RNT (red line), 1% Ag-RNT (green line) and 1.5% Ag-RNT (blue line).

Table 2. Band gap of the photocatalysts determined from the UV-visible spectrum with the Kubelka-Munk function.

Entry	Catalyst	Bandgap (eV)
1	RNT	2.91
2	0.5% Ag-RNT	2.91
3	1% Ag-RNT	2.95
4	1.5% Ag-RNT	2.98

Transmission Electron Microscopy

The nanotubular morphology is clearly observed on the TEM (Transmission Electron Microscopy) images of the 1% Ag-RNT catalyst (Figure 3). The NTs present dimensions of several hundreds of nanometers in length with an external diameter of about 8 nm and a wall thickness of 2 nm, leading to an internal diameter of about 4 nm. This important length/width ratio shows the potential for a higher photocatalytic activity of the as prepared RNTs, as the recombination rate of

the e^-/h^+ pairs should be lower, compared to spherical TiO_2 particles for instance. The isolated Ag particles are quite small and well dispersed on the material with a mean size value of 4 nm.

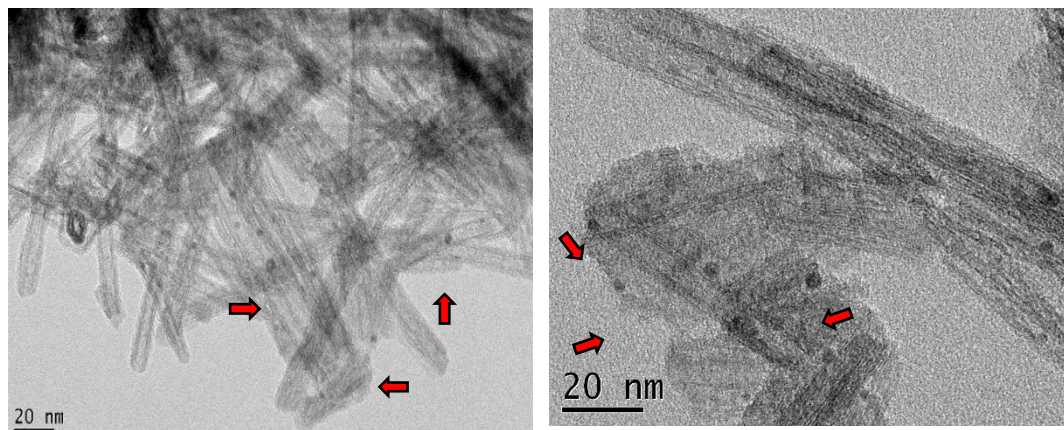
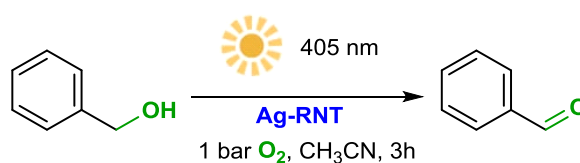


Figure 3. TEM images of 1% Ag-RNT, with arrows pointing some Ag NPs.

Photocatalytic performances in the oxidation of primary alcohols

To characterize the prepared Ag-RNT materials in terms of catalytic performances, the visible-light photo-activities of the materials were evaluated in the selective oxidation of benzyl alcohol into benzaldehyde as a model reaction under 405 nm in the presence of molecular oxygen as oxidant (Scheme 1).

and selectivity into
monitored by Gas



The reaction conversion
benzaldehyde were
Chromatography.

Scheme 1. Photocatalytic oxidation of benzyl alcohol with Ag-doped rutile nanotubes.

In a first set of experiments, the influence of the support (commercially available rutile vs. the as synthesized rutile nanotubes), as well as the amount of silver deposited on RNTs, was studied (Figure 4). In all cases, a complete selectivity towards the benzaldehyde was achieved. Moreover, it is noteworthy to underline that under an argon atmosphere, no reaction occurs with complete recovery of the starting alcohol.

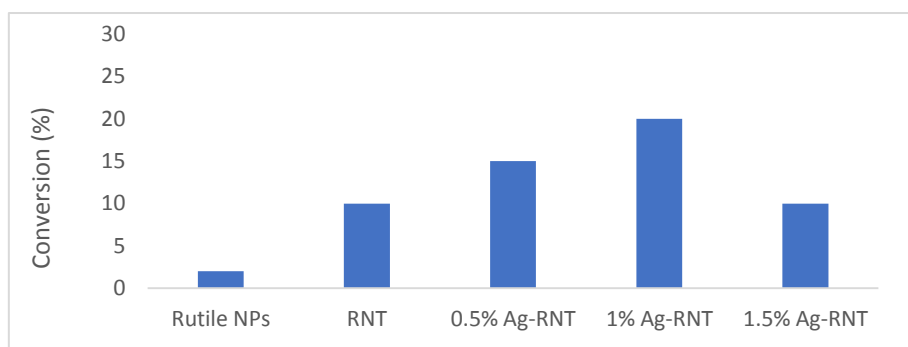
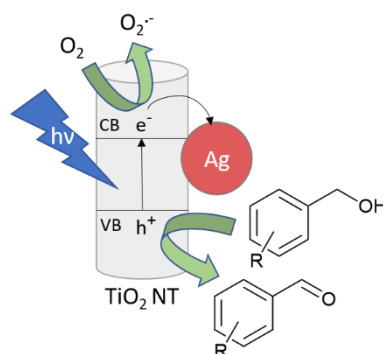


Figure 4. Influence of the support and amount of Ag on the selective oxidation of benzyl alcohol into benzaldehyde.

Reaction conditions: 5 mg catalyst, 0.325 mmol benzyl alcohol, 5 mL acetonitrile, 1 bar O₂, 405 nm, 3 h.

Conversion determined by Gas Chromatography with chlorobenzene as internal standard.

First, after 3 h of irradiation, the synthesized RNTs displayed a better photocatalytic activity than the commercially available rutile NPs (Figure 4) with 10 % of conversion vs. only 2 % for the latter, thus proving the benefits of the nanotube morphology on the catalytic performances. Moreover, doping the RNT with 1% wt. silver (1% Ag-RNT) proves also beneficial to increase by two-fold the conversion rate up to 20 % under the same irradiation time, due to the formation of a Schottky junction that increases the photocatalytic activity of the material (Scheme 2).^[16] However, a higher amount of metal seems to inhibit the activity since only 10% conversion rate was achieved with the 1.5% Ag-RNT photocatalyst. This result could be attributed to a less evenly distribution of active metal in the support,^[17] due to the tendency of Ag NPs to agglomerate at this higher loading, or to a poisoning effect of the active sites of the supporting material, since the TiO₂ photoactive sites can be blocked by an increased silver amount. Moreover, the 1% Ag-RNT catalyst possesses a slightly higher specific surface area compared to other prepared catalysts, thus justifying its enhanced photocatalytic activity. These results indicate that changes in the structure and surface properties of the rutile nanotubes combined with doping with silver have a significant impact on the photocatalytic activity of the obtained materials.



Scheme 2. General mechanism for the photocatalytic oxidation of benzyl alcohol with Ag-doped rutile nanotubes.

Consequently, considering its higher photo-activity, the 1% Ag-RNT was selected for the following experiments. The kinetics of the oxidation reaction has also been studied for 14 h (Figure 5). The selectivity into the targeted aldehyde product was maintained all over the reaction. A slight decrease was only observed after 14 h of irradiation, with a 96 % selectivity at 46 % conversion, owing to the over-oxidation of benzaldehyde into benzoic acid (Figure 5).

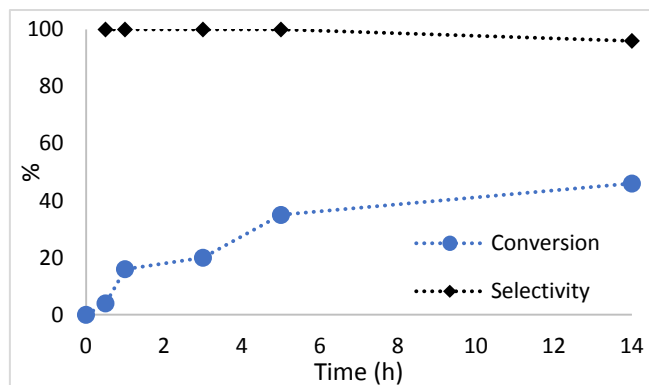
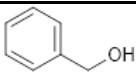
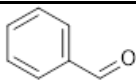
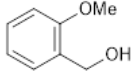
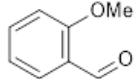
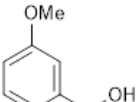
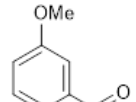
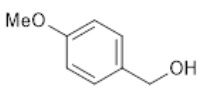
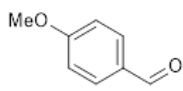
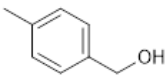
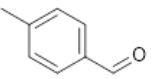
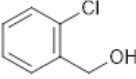
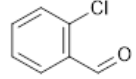
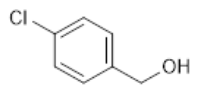
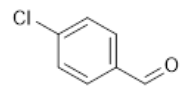
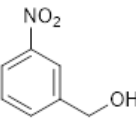
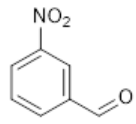
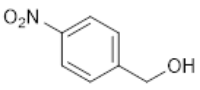
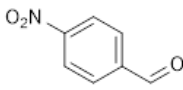
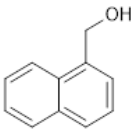
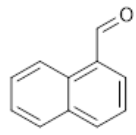
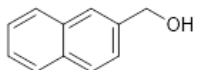
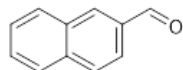


Figure 5. Kinetics of benzyl alcohol oxidation over 1% Ag-RNT photocatalyst.

Reactions conditions: 5 mg catalyst, 0.325 mmol benzyl alcohol, 5 mL acetonitrile, 1 bar O₂, 405 nm. Conversion and selectivity determined by Gas Chromatography with chlorobenzene as internal standard.

Subsequently, to investigate the general applicability of the 1% Ag-RNT material, the scope of the reaction (Table 3) was extended to benzyl alcohol derivatives (Entries 1-9), presenting various electron-donating (-CH₃, -OCH₃) or electron-withdrawing (-NO₂, -Cl) groups on the different positions of the phenyl ring, as well as naphthalene methanol isomers (Entries 10-11). In the benzyl alcohol derivatives series, whatever the substituent is, high levels of selectivity (superior to 95%) were achieved under controlled conversion. Concerning the different substitution positions on the oxidation of the alcohol (*o*-, *m*-, *p*-), better conversions were generally achieved with the *p*-substituted substrate, possibly due to lower steric hindrance. Moreover, no real correlation between the electronic effect of the substituent and the catalytic activity was observed. In the case of both naphthalene derivatives (Entries 10-11), higher levels of conversion were achieved from 34% to 56%, but with lower selectivity for the aldehyde product of only 68 % and 76 %.

Table 3. Photocatalytic oxidation of different benzyl alcohol derivatives with 1% Ag-RNT.

Entry	Substrate	Product	Conv. (%)	Sel. (%)
1			20	>99
2			16	97
3			6	98
4			18	98
5			9	>99
6			8	95
7			15	>99
8			5	96
9			16	98
10			56	68
11			34	76

Reactions conditions: 5 mg catalyst, 0.325 mmol alcohol, 5 mL acetonitrile, 1 bar O₂, 405 nm, 3 h. Conversion and selectivity determined by Gas Chromatography with chlorobenzene as internal standard.

Conclusion

The rutile nanotubes were easily synthesized through an hydrothermal methodology, doped with silver using a wetness impregnation approach and characterized by various analytical techniques. They were investigated in the oxidation of benzyl alcohol as a model reaction in presence of molecular dioxygen and under visible light irradiation, thus showing the beneficial effect of silver on the photocatalytic performances. Best results in terms of catalytic activity (up to 20% conversion), with complete selectivity towards the aldehyde, were achieved with the 1% Ag doped-rutile nanotubes and could be supported by different characterization techniques. In fact, TEM images showed well-defined silver particles that are well-dispersed on the nanotubes surface, combined with an increased BET surface, compared to the other catalytic materials. Moreover, the material is also of good applicability for the oxidation of other primary benzyl alcohols.

Experimental Section

Materials

All the organic compounds were purchased from Acros Organics (Illkirch, France), TCI Europe N.V. (Paris, France), or Sigma-Aldrich (Saint-Quentin-Fallavier, France). Silver nitrate (AgNO_3) was purchased from Acros Organics (Illkirch, France). Sodium hydroxide and hydrochloric acid were purchased from VWR (Rosny-sous-Bois, France) and Fisher Scientific (Illkirch, France). The rutile allotropic form of titanium dioxide was obtained from Sigma-Aldrich (Saint-Quentin-Fallavier, France). Oxygen (Alphagaz™, $\text{O}_2 \geq 99.995\%$) was purchased from Air Liquide (Paris, France). Organic solvents were all HPLC grade. All these starting materials were used without further purification. Water was distilled twice before use by conventional method. The LED lamp was purchased from HepatoChem (EvoluChem™ LED; wavelength: 405 nm; 18W).

Synthesis of the Ag doped rutile nanotubes

Titanate nanotubes were elaborated *via* an alkaline hydrothermal method. 3 g of rutile TiO_2 powder were dispersed into 90 mL of a sodium hydroxide solution (11.25 mol.L^{-1}) in a 150 mL PTFE-line Parr reactor at 130 °C for 20 h at a heating rate of 2 °C/min. The obtained suspension was filtered, and the resulting powder was neutralized with a 0.1 M HCl solution, then washed with hot distilled water several times. The resulting powder of hydrogenotitanate was dried at 80 °C for 12 h. Samples are named RNT for Rutile Nanotubes.

The as prepared RNT were doped with different amounts of silver (0.5, 1 and 1.5 wt %), and respectively denoted 0.5% Ag-RNT, 1% Ag-RNT and 1.5% Ag-RNT, using an incipient wetness

impregnation method. The desired amount of silver nitrate (AgNO_3) used as silver precursor was dissolved in a minimum volume of Milli-Q water (equivalent to twice porous volume of RNT). Then the adequate quantity of RNT was added under stirring for 2 h. The obtained material was dried in an oven at 80 °C for 24 h.

Rutile-NT characterization

The chemical composition of the Ag-RNT photocatalysts has been determined by Inductively Coupled Plasma Optical Emission Spectrometry (ICP-OES). About 10 mg of the catalyst were mixed with 0.5 mL of regal water (HCl/HNO_3 , 3/1), and heated for 16 h at 40 °C. The sample was diluted in 25 mL of distilled water, and quantified by ICP-OES with an iCAP 7000Series Thermo Scientific device.

Textural properties of the different photocatalysts were obtained on a Autosorb AS-1 from Quantachrome Instruments, using N_2 adsorption-desorption isotherms at 77 K. Specific surface areas were obtained using the Brunauer-Emmett-Teller (BET) method and the ASiQwin software, considering the adsorption data branch in the relative P/P0 pressure range varying between 0.05 and 0.25.

The photocatalysts were structurally characterized by powder X-ray diffraction at room temperature on a Panalytical Empyrean powder diffractometer (θ - θ Bragg-Brentano geometry) with Cu $\text{K}\alpha$ nickel filtered radiation ($\lambda \text{K}\alpha_1=1.5406 \text{ \AA}$; $\lambda \text{K}\alpha_2=1.5444 \text{ \AA}$) selected with a flat multilayer X-ray mirror (Bragg-Brentano HD[®]).

Diffuse reflectance measurements were carried out in a Jasco UV-vis diffuse reflectance spectrophotometer equipped with an integrating sphere reflectance unit. The reflectance data (R) were converted to the Kubelka-Munk (K-M) function, $F(R) = \alpha = (1-R)^2/2R$. The band gap energy values were obtained from the K-M vs photon energy plot.

The nanomorphology of the Ag-RNT samples were studied by High-Resolution Transmission Electron Microscopy (HRTEM). Images were acquired on a JEOL JEM-2100 (200 kV) microscope to determine the shape of the different titania samples and the particle sizes of the Ag NPs. Before analysis, ethanol was first used to disperse the samples.

Photocatalytic tests

The selective photocatalytic oxidation of various benzyl alcohol derivatives was performed as follow. Typically, a solution of alcohol (0.065 mol/L) in acetonitrile (5 mL) and 5 mg of the catalyst were stirred under O_2 atmosphere (1 bar) in a glass tube, and irradiated by a LED at 405 nm. After the reaction, the suspension was filtered through a 0.20 μm syringe filter to remove the catalyst. The

solution was then analyzed by Gas Chromatography analysis with chlorobenzene as internal standard. Conversion of alcohol and selectivity for the aldehyde product were determined with the following equations:

$$\text{Conversion (\%)} = ((C_0 - C_{\text{alcohol}})/C_0) * 100$$

$$\text{Selectivity (\%)} = C_{\text{aldehyde}} / (C_0 - C_{\text{alcohol}}) * 100$$

C_0 : initial alcohol concentration

C_{alcohol} : final alcohol concentration

C_{aldehyde} : final aldehyde concentration

Acknowledgements

The authors are grateful to Bertrand Lefeuvre from UMR-CNRS 6226, Université de Rennes 1 for ICP analysis and to Sandra Casale from the Service de Microscopie Electronique at Fédération de Chimie et Matériaux de Paris-Centre FCMat - Sorbonne Université for Transmission Electron Microscopy analyses and discussions.

Conflict of interest

The authors declare no conflict of interest.

Keywords

Rutile Nanotubes • Silver • Visible light • Selective Oxidation of Benzyl Alcohol

References

- [1] I. Ali, M. Suhail, Z. A. Alothman, A. Alwarthan, *RSC Adv.* **2018**, *8*, 30125–30147.
- [2] J. Wang, Z. Wang, W. Wang, Y. Wang, X. Hu, J. Liu, X. Gong, W. Miao, L. Ding, X. Li, J. Tang, *Nanoscale* **2022**, *14*, 6709–6734.
- [3] A. H. Mamaghani, F. Haghghat, C.-S. Lee, *Appl. Catal., B* **2020**, *269*, 118735.
- [4] P. Roy, S. Berger, P. Schmuki, *Angew. Chem., Int. Ed.* **2011**, *50*, 2904–2939.
- [5] R. Savitha, R. Raghunathan, R. Chetty, *Appl. Surf. Sci.* **2023**, *609*, 155252.
- [6] Y. Wen, B. Liu, W. Zeng, Y. Wang, *Nanoscale* **2013**, *5*, 9739–9746.
- [7] C. Nutescu Duduman, C. Gómez de Castro, G. A. Apostolescu, G. Ciobanu, D. Lutic, L. Favier, M. Harja, *Water* **2022**, *14*, 2711.
- [8] R. Gang, Y. Xia, L. Xu, L. Zhang, S. Ju, Z. Wang, S. Koppala, *Surf. Interfaces* **2022**, *31*, 102018.

- [9] S. I. Mogal, V. G. Gandhi, M. Mishra, S. Tripathi, T. Shripathi, P. A. Joshi, D. O. Shah, *Ind. Eng. Chem. Res.* **2014**, *53*, 5749–5758.
- [10] D. Wodka, E. Bielańska, R. P. Socha, M. Elźbieciak - Wodka, J. Gurgul, P. Nowak, P. Warszyński, I. Kumakiri, *ACS Appl. Mater. Interfaces* **2010**, *2*, 1945–1953.
- [11] S. Yurdakal, G. Palmisano, V. Loddo, V. Augugliaro, L. Palmisano, *J. Am. Chem. Soc.* **2008**, *130*, 1568–1569.
- [12] F. Parrino, M. Bellardita, E. I. García-López, G. Marci, V. Loddo, L. Palmisano, *ACS Catal.* **2018**, *8*, 11191–11225.
- [13] A. Kumar, P. Choudhary, V. Krishnan, *Appl. Surf. Sci.* **2022**, *578*, 151953.
- [14] E. Pulido Melián, O. González Díaz, J. M. Doña Rodríguez, G. Colón, J. A. Navío, M. Macías, J. Pérez Peña, *Appl. Catal. B* **2012**, *127*, 112–120.
- [15] D. Zhang, S. Dong, *Prog. Nat. Sci.: Mater.* **2019**, *29*, 277–284.
- [16] L. Xiong, J. Tang, *Adv. Energy Mater.* **2021**, *11*, 2003216.
- [17] S. Wang, S. A. Nabavi, P. T. Clough, *Int. J. Hydrogen Energy* **2023**, *48*, 15879–15893.